Entropically Induced Euler Buckling Instabilities in Polymer Crystals

Mark R. McGann and Daniel J. Lacks

Department of Chemical Engineering, Tulane University, New Orleans, Louisiana 70118
(Received 31 August 1998)

Molecular simulations show that heating crystalline polyethylene leads to an entropically induced Euler buckling instability, associated with the softening of the long wavelength transverse acoustic vibrational modes propagating along the chain axis. This entropic effect is augmented by axial compressive stress, leading to a decrease in the instability temperature with applied stress. For zero or low compressive stresses, the instability will occur above the melting temperature and impose a maximum temperature for the superheated crystal; for high compressive stresses, the instability will occur below the melting temperature and trigger a transition to another solid structure. [S0031-9007(98)08367-7]

Instabilities of crystals, and the associated destabilization mechanisms, are phenomena of some interest. The application of pressure leads to amorphization in systems such as silica [1] and ice [2], which have been explained in terms of mechanical instabilities in the crystal [3–6]. Similarly, the application of uniaxial stress can lead to material failure, which has been explained in many instances in terms of underlying crystal instabilities [7–11]. Thermally induced mechanical instabilities can lead to solid-solid phase transitions if occurring below the melting temperature [12,13], or impose a maximum temperature limit for superheated crystals if occurring above the melting temperature [11,14–18].

Previous studies of mechanical instabilities in crystals have usually focused on simple nonmolecular crystals. The behavior of polymer crystals can be very different, due to the extreme anisotropy in these systems. We have previously shown that material failure in extended-chain polymer crystals under axial compression (i.e., along the polymer chain axis) proceeds through mechanical instabilities corresponding to Euler buckling, which is unique to long chain systems [9,10]. The present work addresses the temperature limits of stability in polymer crystals under stress.

Molecular simulations are used to examine the stability of crystalline polyethylene as a function of temperature and axial stress. The force field of Karasawa *et al.* [19] is used, which explicitly models all atoms and leads to accurate vibrational frequencies (qualitatively similar results were also obtained with the force field of Palmo *et al.* [20]); Ewald methods are used to sum the long range Coulombic and dispersion interactions. Thermal effects are incorporated with lattice dynamics. A single unit cell is explicitly modeled, and Fourier space methods are used to account for vibrations occurring over more than one unit cell (the unit cell is orthorhombic for polyethylene). The unit cell dimensions are obtained as those that minimize the Gibbs free energy, which is evaluated as the sum of the potential energy, stress-strain energy, and vibra-

tional free energy obtained in the quasiharmonic approximation (using the quantum mechanical partition function). This method is described in detail elsewhere and is shown to give very good results for polyethylene over a fairly wide temperature range [21,22].

The lattice dynamics approach is used due to its efficiency in accounting for long wavelength motions in Fourier space; these long wavelength modes are important in regards to the stability of a polymer crystal [9,10]. Direct-space methods, such as molecular dynamics, would require extremely large simulation cells to capture these effects. A disadvantage of the lattice dynamics approach is that it cannot determine the outcome of an instability (but only when an instability occurs). Also, at temperatures near the stability limit there may be significant quantitative error associated with the quasiharmonic approximation, but as discussed below, we feel that the qualitative picture that emerges is nonetheless correct.

The results for the unit cell dimensions are shown in Fig. 1 as a function of temperature, at zero pressure and zero axial stress. As the temperature is increased, the unit cell area perpendicular to the chain axis increases while the lattice parameter parallel to the chain axis decreases. The negative thermal expansion along the chain axis has previously been explained as an entropic effect arising from the increased motion perpendicular to the chain axis that is allowed as the lattice parameter along the chain axis decreases [23], specifically, this motion is associated with the transverse acoustic mode (TAM) propagating along the chain axis, shown schematically in Fig. 2. A stable crystal structure could not be obtained above $\sim$480 K, because the free energy minimum corresponding to the crystal structure no longer exists.

The disappearance of a free energy minimum, at zero pressure and stress, is associated with the elastic stiffness matrix becoming nonpositive definite. The stiffness matrix, in Voigt notation, is a 6×6 matrix with components $C_{ij} = (1/V)(\partial^2 A/\partial \varepsilon_i \partial \varepsilon_j)$, where A is the Helmholtz free energy, V is the volume, and ε_i is the strain ($\varepsilon_1 - \varepsilon_3$ are the
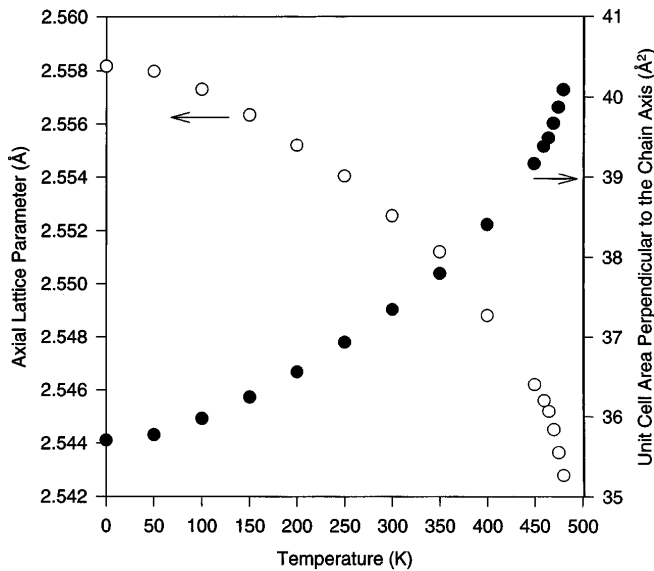
FIG. 1. Unit cell dimensions as a function of temperature. Open circles: parallel to chain axis; closed circles: perpendicular to the chain axis.

strains with respect to the orthorhombic lattice parameters with ε_3 being along the chain axis, and $\varepsilon_4 - \varepsilon_6$ are the shear strains). As shown in Fig. 3, the increase in temperature leads to decreases in C_{11}, C_{22}, C_{33}, and C_{21} but increases in C_{31} and C_{32}. These changes in the stiffness moduli cause an eigenvalue of the stiffness matrix to decrease to zero as $T \rightarrow 480$ K; the eigenvector associated with this eigenvalue indicates that the instability involves increases in ε_1 and ε_2 coupled with a decrease in ε_3.

A normal mode analysis shows that this instability is driven by the softening of the long wavelength TAMs which propagate along the chain axis, with Brillouin zone
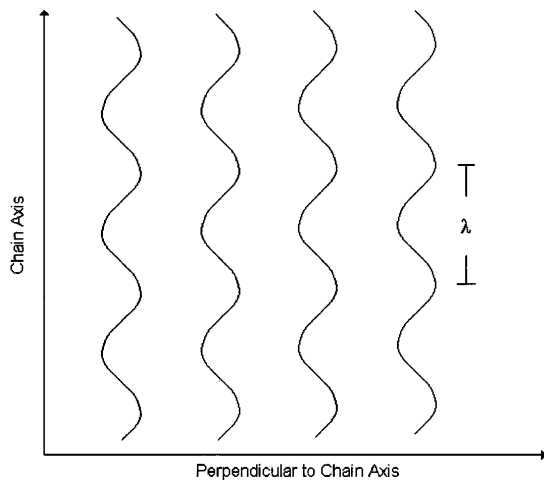

FIG. 2. Schematic of the $k_1 = k_2 = 0$ transverse acoustic vibrational modes which propagate along the chain axis. The wavelength of the vibration is $\lambda = 2\pi/k_3$. Note that $k_1 = k_2 = 0$ implies that all chains vibrate in phase.
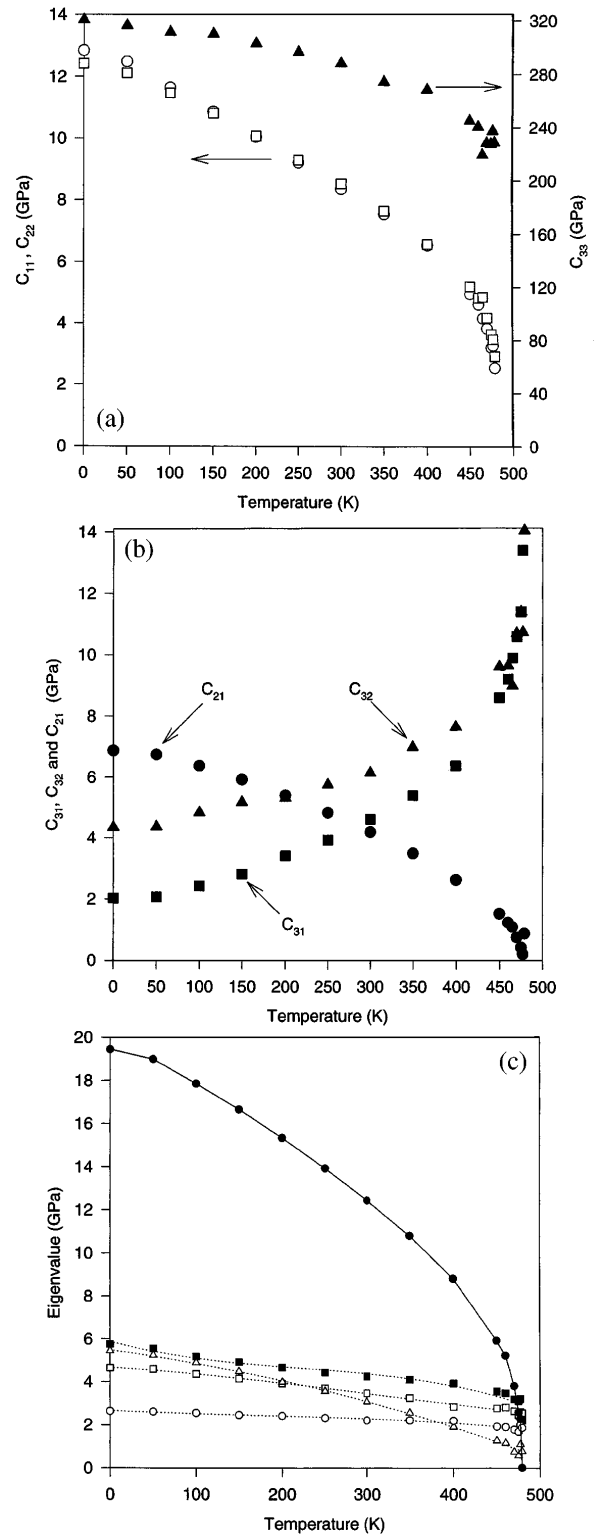

FIG. 3. Results for the stiffness matrix as a function of temperature: (a) Orthorhombic diagonal components; (b) orthorhombic off-diagonal components; (c) eigenvalues of the stiffness matrix. The corresponding eigenvectors are as follows: closed circles ($\varepsilon_1 > 0, \varepsilon_2 > 0, \varepsilon_3 < 0$); closed squares ($\varepsilon_1 < 0, \varepsilon_2 > 0, \varepsilon_3 < 0$); open circles ($C_{44}$); open squares ($C_{55}$); open triangles ($C_{66}$). The eigenvalue corresponding to ($\varepsilon_1 > 0, \varepsilon_2 > 0, \varepsilon_3 > 0$) is not shown because it has a value greater than 250 GPa at all temperatures.

wave vectors $k_1 \approx 0$, $k_2 \approx 0$, and $k_3 \rightarrow 0$. These TAM frequencies are decreased most significantly by the strain combination ($\varepsilon_1 > 0, \varepsilon_2 > 0, \varepsilon_3 < 0$), because both the increase in the cross-sectional area per chain and the decrease in the lattice parameter along the chain axis allow for more motion perpendicular to the chain axis. The effects of these strains are coupled (entropically), leading to the increase in C_{31} and C_{32} and the decrease in C_{21} with temperature.

The present instability, which occurs as polymer crystals are heated, is somewhat analogous to the tetragonal shear instability which occurs as cubic crystals are heated [11,14]. The two instabilities are characterized by the same strain combination ($\varepsilon_1 > 0, \varepsilon_2 > 0, \varepsilon_3 < 0$) and arise from similar changes in the stiffness matrix (i.e., the decrease in C_{11}, C_{22}, and C_{33} and increases in C_{31} and C_{32} which lead to the present instability are comparable to the decrease of $C_{ii} - C_{ij}$ ($j \neq i$) which leads to the tetragonal shear instability).

Equilibrium along the axial direction implies that $\partial G/\partial \varepsilon_3 = 0$, where the Gibbs free energy $G = \phi + U^{\text{vib}} - TS - V\varepsilon_3 \sigma_3^{\text{app}}$, ϕ is the potential energy, U^{vib} is the vibrational energy, S is the entropy, and σ^{app} is the applied stress. Thus, the condition for equilibrium can be considered as

$$\frac{1}{V}\frac{\partial \phi}{\partial \varepsilon_3} - (\sigma_3^{\text{vib}E} + \sigma_3^{\text{ent}} + \sigma_3^{\text{app}}) = 0, \qquad (1)$$

where $\sigma_3^{\text{vib}E} = -(1/V)(\partial U^{\text{vib}}/\partial \varepsilon_3)$ and $\sigma_3^{\text{ent}} = (T/V)(\partial S/\partial \varepsilon_3)$. The results of athermal continuum models [24] and molecular simulations [9,10] have shown that the ($k_1 = 0$, $k_2 = 0$, $k_3 \rightarrow 0$) TAM frequency becomes imaginary for $(1/V)(\partial \phi/\partial \varepsilon_3) > G$, where G is the lowest value of the second derivative of the potential energy with respect to shear strain in a plane that includes the chain axis (for polyethylene, $G = \partial^2 \phi/\partial \varepsilon_5^2$). Since $\sigma_3^{\text{vib}E} = \sigma_3^{\text{ent}} = 0$ for the athermal case, this TAM frequency becomes imaginary in athermal systems for $(-\sigma_3^{\text{app}}) > G$ [9,10,24]. The soft mode instability of this TAM corresponds to Euler buckling.

For thermal systems in the absence of applied stress, the TAM frequency becomes imaginary for $-(\sigma_3^{\text{vib}E} + \sigma_3^{\text{ent}}) > G$. As discussed previously [21], the values of σ_3^{ent} and $\sigma_3^{\text{vib}E}$ in polyethylene are characterized by $\sigma_3^{\text{ent}} < 0$ and $\sigma_3^{\text{vib}E} > 0$ ($\sigma_3^{\text{vib}E}$ is due to quantum effects and equals zero with classical mechanics). At high temperatures the effects of σ_3^{ent} dominate and move the system towards a soft mode instability. Note that a mechanical instability involving changes in the lattice parameters will precede a vibrational instability (which corresponds to fixed lattice parameters). As shown in Fig. 4, the instability does in fact occur just before $-(\sigma_3^{\text{vib}E} + \sigma_3^{\text{ent}})$ reaches G.

These entropically induced stresses are augmented by applied compressive stresses, because σ_3^{ent} and σ_3^{app}
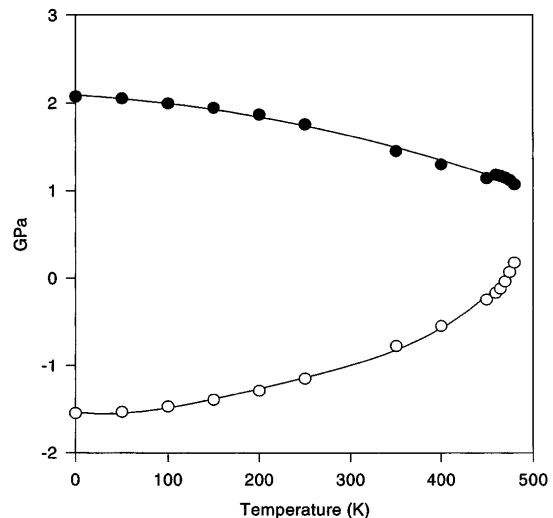

FIG. 4. G (closed circles) and $-(\sigma_3^{\text{vib}E} + \sigma_3^{\text{ent}})$ (open circles) as a function of temperature.

are both negative. The condition $-(\sigma_3^{\text{app}} + \sigma_3^{\text{vib}E} + \sigma_3^{\text{ent}}) < G$ necessary for the crystal to be stable thus implies that the instability temperature will decrease with increasing compressive stress and approach zero as $-(\sigma_3^{\text{app}} + \sigma_3^{\text{vib}E})$ approaches G. We therefore carried out finite stress simulations, in which the instability temperature is determined as the highest temperature for which the free energy minimization yields a stable crystal structure (this method avoids the finite-stress complications associated with the instability criteria based on the stiffness matrix [25]). Our simulation results, shown in Fig. 5, exhibit the predicted decrease of the instability temperature with increasing applied axial compressive stress.

When the crystal is heated at low applied stresses, the instability will occur at temperatures above the melting temperature and will thus trigger melting of the superheated cycle as in other systems [15–18]. The atomic motions and unit cell distortions which accompany the instability can be construed as the initiation of chain coiling. However, as the applied stress becomes large enough, the instability temperature will decrease to a value below the melting temperature; the instability will now trigger a transition to another solid structure, similarly to other systems [12,13]. (There is presumably another crystal structure which becomes thermodynamically stable, but the transformation to this structure will most likely be kinetically hindered; the result of the instability is therefore likely to be a disordered structure.)

These results present a simple picture of the thermal stability of extended chain polymer crystals which we feel is valid beyond the approximations used in the simulations. This simple picture is that temperature generates an entropically induced axial compressive stress that is entirely analogous to an applied compressive stress; this axial compressive stress leads to axial contraction of the
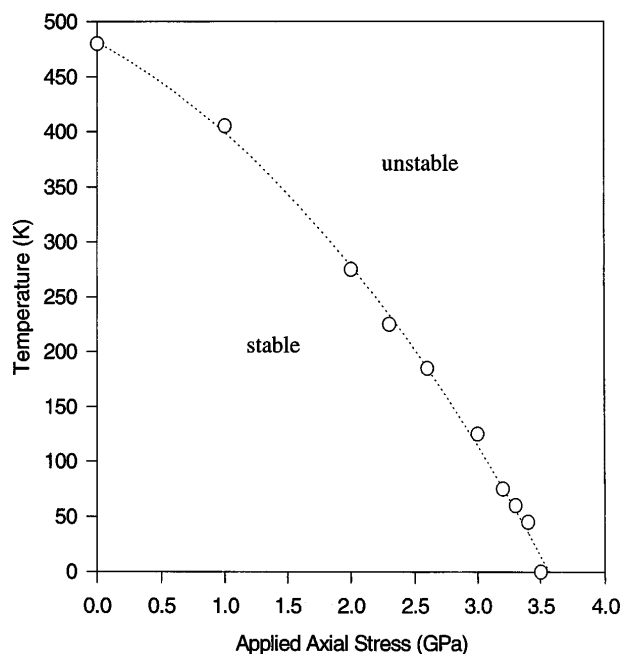
FIG. 5. The instability temperature as a function of applied stress.

crystal, which in turn can lead to a mechanical instability. An applied compressive stress will augment the entropically induced stress, causing the instability temperature to decrease to zero as the applied stress increases. Evidence of the validity of this simple picture is that the separate parts of this picture concur with experiment: The result that temperature leads to an entropically induced compressive stress concurs with the observed axial thermal contraction in polymer crystals [23], and the result that axial contraction leads to mechanical instabilities concurs with the material failure observed in polymer fibers under axial compression [24]. Regarding the quasiharmonic approximation, tests on simple systems show that this approximation gives qualitatively correct results (in comparison with molecular dynamics results) for thermal expansion up to the instability point, even though the magnitude of thermal expansion becomes increasingly overestimated [26]; the quasiharmonic approximation is thus expected to give a quantitative underestimate of the instability temperature, but not to invalidate the qualitative picture described above. We note that direct-space methods (e.g., molecular dynamics) could be used to simulate the instability, but will overestimate the stress and/or temperature necessary to induce Euler buckling instabilities due to finite system size (the stress for an instability $\approx A + B/(\text{system length})^2$, where A and B are constants) [9,10,24].

The present results are expected to apply to all polymer crystals composed of extended chain polymers. The importance of these results is that such polymer crystals comprise the polymer fibers used in many composite materials, and these composite materials are often used in structural applications under external stresses and elevated temperatures.

[1] R. J. Hemley, A. P. Jephcoat, H. K. Mao, L. C. Ming, and M. H. Manghnani, Nature (London) **334**, 52 (1988).
[2] O. Mishima, L. D. Calvert, and E. Whalley, Nature (London) **310**, 393 (1984).
[3] J. S. Tse, J. Chem. Phys. **96**, 5482 (1992).
[4] J. S. Tse and D. D. Klug, Phys. Rev. Lett. **67**, 3559 (1991).
[5] M. Tang and S. Yip, Phys. Rev. Lett. **75**, 2738 (1995).
[6] N. Binggeli and J. R. Chelikowsky, Phys. Rev. Lett. **69**, 2220 (1992).
[7] M. Tang and S. Yip, J. Appl. Phys. **76**, 2719 (1994).
[8] F. Cleri, J. Wang, and S. Yip, J. Appl. Phys. **77**, 1449 (1995).
[9] D. J. Lacks, J. Mater. Sci. **31**, 5885 (1996).
[10] M. R. McGann and D. J. Lacks, Macromolecules **31**, 6356 (1998).
[11] J. Wang, S. Yip, S. R. Phillpot, and D. Wolf, Phys. Rev. Lett. **71**, 4182 (1993).
[12] W. Cochran, Adv. Phys. **9**, 387 (1960).
[13] P. A. Fleury, J. F. Scott, and J. M. Worlock, Phys. Rev. Lett. **21**, 16 (1968).
[14] J. Wang, J. Li, S. Yip, D. Wolf, and S. Phillpot, Physica (Amsterdam) **240A**, 396 (1997).
[15] M. Born, J. Chem. Phys. **7**, 591 (1939).
[16] L. L. Boyer, Phys. Rev. Lett. **42**, 584 (1979); **45**, 1858 (1980).
[17] J. L. Tallon, Nature (London) **342**, 658 (1989).
[18] H. J. Fetch and W. L. Johnson, Nature (London) **334**, 50 (1988).
[19] N. Karasawa, S. Dasgupta, and W. A. Goddard, J. Chem. Phys. **95**, 2260 (1991).
[20] K. Palmo, N. G. Mirkin, and S. Krimm (to be published).
[21] D. J. Lacks and G. C. Rutledge, J. Phys. Chem. **98**, 1222 (1994).
[22] G. C. Rutledge, D. J. Lacks, R. Martonak, and K. Binder, J. Chem. Phys. **108**, 10 274 (1998).
[23] Y. Kobayashi and A. Keller, Polymer **11**, 114 (1970).
[24] S. DeTeresa, R. Porter, and R. J. Farris, J. Mater. Sci. **20**, 1645 (1985).
[25] J. Wang, J. Li, S. Yip, S. Phillpot, and D. Wolf, Phys. Rev. B **52**, 12 627 (1995).
[26] For example, D. J. Lacks and R. C. Shukla, Phys. Rev. B **54**, 3266 (1996).